Proceedings of 2013 IEEE
International Conference on Mechatronics and Automation
August 4 - 7, Takamatsu, Japan

Performance Evaluation on Land of an Amphibious Spherical Mother Robot in Different Terrains

Shuxiang Guo[1,3], Maoxun Li [2,3], Chunfeng Yue[2]
[1]*Faculty of Engineering, Kagawa University, Japan*
[2]*Graduate School of Engineering, Kagawa University, Japan*
[3]*Harbin Engineering University, China*
guo@eng.kagawa-u.ac.jp, s12g537@stmail.eng.kagawa-u.ac.jp

Abstract - **In recent years, a variety of underwater microrobots were applied widely to underwater operations in limited spaces. The robots had some limitations of locomotion velocity and enduring time because of their compact structures. For solving these problems, we proposed a mother-son robot cooperation system and designed a novel amphibious spherical robot as the mother robot to carry the microrobots as son robots for collaboration. The spherical mother robot consisted of a sealed hemispheroid, two openable quarter spherical shells, a plastic circular plate, a plastic shelf for carrying microrobots and four actuating units. Each unit was composed of a water jet propeller and two servo motors, each of which could rotate 90° in horizontal or vertical direction respectively. The robot could implement on-land locomotion, as well as underwater locomotion. In this paper, a prototype spherical mother robot was developed and three walking gaits, decided by the duty factory, were designed for the on-land motion of the robot. Then the walking experiments were carried out in different terrains for evaluating the performance of the robot. From the results, the robot has a higher walking performance on tile floor. Under a control frequency of 3.33 Hz in Gait 3, we got a maximal walking velocity of 22.5 cm/s. For climbing performance, Gait 2 has the best performance on a steep slope with the inclination angle of 8°.**

Index Terms – Spherical robot, Amphibious robot, Quadruped walking, Mother robot, Walking gait.

I. INTRODUCTION

Underwater robots have been widely used in submarine topography survey, pipeline cleaning, water samples collection, and recovering underwater objects for several years. However, it is hard for normal underwater robots to do operations in limited spaces. For having the compact structure, microrobots actuated by smart actuators including ICPF actuators [1]-[6] and SMA actuators [7]-[9] are utilized to work in narrow spaces. Nevertheless, the compact structure also brings limited multi-functionality, locomotion velocity and enduring time to microrobots. Microrobots usually have a lower speed because of the properties of the smart actuators. And it is difficult for the wireless microrobots to achieve a long enduring time by a compact structure, with which the robot is unable to carry large power supply. For wire microrobots, they can get enough energy supply from power supply through the cable, but at the same time limited in the range of movement.

In this paper, we proposed a mother-son robot cooperation system to solve the problems mentioned above. A mother robot can carry son robots to a proper place near the target firstly during the operations under the water. When getting close to the target or encountering a narrow space that the mother robot cannot get through, it will reel out the son robots to get the target. A mother robot, which carried the power supply and the control circuit of the son robots, can provide the power supply to the son robots and control them by cables. Till now, there are fewer researches using this mother-son underwater robot cooperation system. Hence we designed and built a novel amphibious spherical robot as the mother robot to carry the microrobots actuated by ICPF actuators as son robots for collaboration. The spherical robot can move under the water as well as walk on land.

Compared to individual microrobots, mother-son robot system can perform a wide range of movement, by reason of spherical mother robot [10]-[14] having a relatively high moving speed and a long enduring time.

Compared to a single spherical robot, mother-son robot system can be applied in various practical environments, especially limited spaces. Compact structure of the microrobots can also provide a more precise control than spherical robots.

In comparison with other shapes, spherical robot has the maximum inner space. Besides, by having the symmetry, spherical robot has the advantage of flexibility. We proposed the design of the first generation of the spherical robot, which has the compact structure and the large inner space, in 2012. To improve the performance of the spherical robot, we redesigned the size of the structure. In this paper, we designed and developed a novel amphibious spherical mother robot in the first place. And a lot of walking experiments were carried out in different terrains for evaluating the performance of the spherical robot. And also the climbing experiments on a slope were done.

This paper consists of five parts. In section II, we described the structural design of the spherical robot and introduced the motion mechanisms of the robot on the land. Then we proposed three kinds of walking gaits and analyzed the characterization of each gait in section III. And a prototype was given in section IV and experiments were conducted to evaluate the performance of walking velocity in different terrains. And we discussed the results of the experiments. Finally, we drew the conclusions in section V.

978-1-4673-5558-2/13/$31.00 ©2013 IEEE

II. Structural Design Of The Spherical Robot

The mother-son robot cooperation system is composed of an amphibious spherical robot as mother robot and several microrobots as son robots. In order to adapt to different environments, the mode of locomotion of the spherical robot can change between water-jet mode and quadruped walking mode. During the actual operation, the spherical robot moves close to the target first and then keeps still. And microrobots move out of it and get in the narrow spaces like the pipeline to do operation. After finishing the work, microrobots will be taken back to the mother robot.

A. Proposed Spherical Robot Structure

Fig.1 shows the proposed spherical mother robot, which consists of a sealed transparent hemispheroid, two openable transparent quarter spherical shells, a plastic circular plate, a plastic shelf and four actuating units. Several sensors are carried on the sealed hemispheroid with control circuits and batteries to be waterproof. Two servo motors are used to control these two quarter spherical shells to open and close simultaneously. The plastic plate in the lower hemisphere of the robot is set for carrying microrobots. Each actuating unit is made of a water jet propeller and two servo motors. The two servo motors on the same actuating unit are mutually perpendicular, with which each actuating unit can realize two degrees of freedom movement. The diameter of the upper hemisphere is 234 mm and the diameter of the lower hemisphere is 250 mm. The height of actuating unit in standing state is 108 mm, and the length of it is 85 mm.

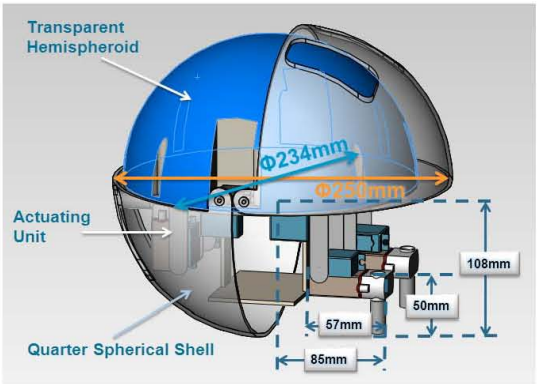

Fig. 1 Spherical mother robot structure

B. Actuating System Mechanisms

As the mechanisms of the actuating system, the spherical mother robot can move both on land and under water. The actuating system consists of four main actuating units. Each unit includes a water jet propeller, two servo motors and a stainless steel stand. The motor connected to the upper hemisphere is controlled to move in horizontal direction. While another motor fixed on the water jet propeller is controlled to move in vertical direction.

For the walking movements on land, actuating units are considered as legs, each of which has two degrees of freedom. The robot can realize walking and rotating motions on land as a quadruped robot. However, under the water, water jet propellers are the main actuators of the robot. By controlling the rotating angles of the servo motors, spray angle of each water jet propeller can be changed to realize the moving forward and backward, rotating, rising and diving motions.

Two servo motors, which are set on the surface of the plastic circular plate outside the upper hemisphere, are used to control the spherical shells open or closed on land and under water.

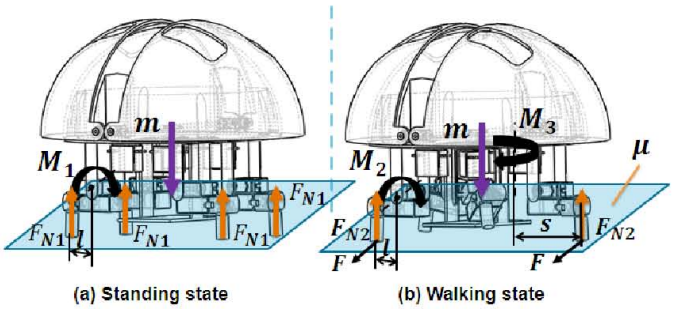

Fig. 2 Force analysis for standing state (a) and walking state (b) on land

In order to choose the appropriate servo motors used on the four legs of the robot, we did the following force analysis and calculations. Fig. 2 shows the on-land force analysis of the robot. When the robot in standing state, each vertical servo motor will be forced on the torque of M_1. And in walking state, each vertical servo motor of the still legs and each horizontal servo motor of the moving legs will be forced on the torque of M_2 and M_3 separately. Here we pretended that in one moment the supporting force forcing on each leg contacting with the ground is the same. Considering that the torque forced on each servo motor cannot exceed its rated torque, M, we did the calculations as follows.

$$mg = 4F_{N1} = 2F_{N2} \tag{1}$$

$$M_1 = F_{N1} \times l \tag{2}$$

$$M_2 = F_{N2} \times l \tag{3}$$

$$M_3 = F \times s = \mu F_{N2} \times s \tag{4}$$

Where: F_{N1}, F_{N2} are the normal force exerted by each surface, F is the force of friction, μ is the friction coefficient of the contact surface, l is the moment arm of vertical motor, s is the moment arm of horizontal motor.

$$\max(M_1, M_2, M_3) < M \tag{5}$$

The upward force of F_N is different depending on the different walking gaits. As equation (1) shows, the force of F_{N1} is the minimal force which supports the ground, when robot stand with four legs. While the robot walks on land, there is an instant that only two legs of the robot contact with

the ground. The supporting force is F_{N2}, which is maximal supporting force. After making sure that equation (5) holds, servo motors are decided.

C. Control System Mechanisms and Batteries

The control center of the spherical robot is AVR ATMEGA2560 micro-controller. We use ten channels of PWM signals to control the eight servo motors on the legs to actuate the robot, and two servo motors on the upper hemisphere to open and close two quarter spherical shells. Use eight Input/output ports to control four water jet propellers for positive rotating and negative rotating motion. Another four Input/output ports are contacted to the remote controller with four channels which controls the movement of the robot.

For the power supply, we use three batteries, one of which, 6TNH22A/8.4 V, is for providing the power to AVR micro-controller, other two of which, YBP216BE/7.4 V, are used to provide the power to ten servo motors and four water jet propellers.

III. Gait Characterization

For adapting to different environments, quadruped robots applied several walking gaits [15]. Three kinds of walking gaits were implemented on the spherical robot. The first walking gait (Gait 1) is a statically stable regular symmetric gait, that in an event φ at least three legs contact with the ground at all times. Accordingly, the gait event sequences and the gait timing sequences can be defined by the duty factor β and the relative phase of the left hind leg φ_{LH}. The relative phases of all the legs are set that φ_{LF} is 0, φ_{RF} is 0.5 and RH has a phase difference of 0.5 with LH. Fig. 3(a) shows the event sequences of the first walking gait following the duty factor β of 0.8.

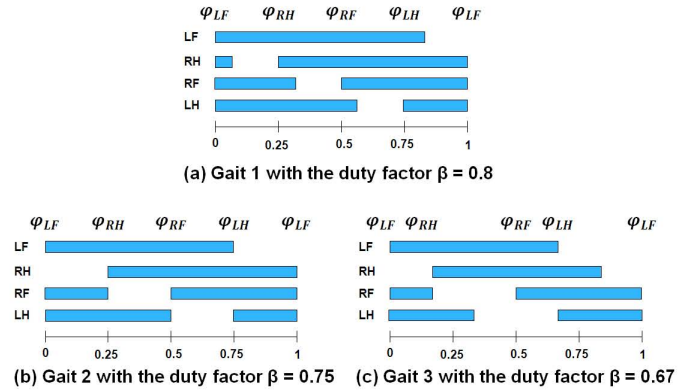

Fig. 3 Event sequences of one step cycle for different gaits. The legs: LF, left foreleg; RF, right foreleg; LH, left hind leg; RH, right hind leg. Blue bars indicate that legs contact with ground.

As Fig. 3(b) and Fig. 3(c) shows, the second and third walking gaits follow a rule that the front leg is lifted while the ipsilateral hind leg is set down, which can achieve a maximal stability margin. The rule means that the relative phase of the left hind leg φ_{LH} follows the duty factor β. The duty factor of the second walking gait is set to 0.75, which can achieve a maximal time of contacting the ground among the walking gaits following the rule. As the speed increases, the duty factor decreases. While the duty factor of the third walking gait is set to 0.67. There is a moment that the robot only uses two legs to support the body.

As equation (6) shows, the velocity of the robot is related to the step size of the robot and frequency of one step cycle. And the step size is in proportion to the rotating angle of the leg which is the rotating angle of the horizontal motor and duty factor of the gait timing sequences, as shown in equation (7). Hence, by plugging equation (7) to equation (6), we can get equation (8), which is related to the frequency and duty factor. of the robot.

$$v = d * f \tag{6}$$

$$d = (\frac{\theta}{180} * \pi * s)/\beta = 0.1483 * \theta/\beta \tag{7}$$

$$v = 0.1483 * \theta * f/\beta \tag{8}$$

Where: v is the velocity of the robot, d is the step size of the robot, f is the frequency of one step cycle, β is the duty factor of the gait timing sequences, θ is rotating angle of the horizontal motor.

IV. Prototype Spherical Robot And Experiments

A. Prototype Spherical Robot

A prototype amphibious spherical mother robot was made with quadruped walking mode and water-jet mode, as shown in Fig. 4. The robot consists of two main parts, the upper hemisphere and two transparent quarter spherical shells. The actuating system and the plastic shelf for microrobots were set in the lower hemisphere. We chose to use HS-5086WP waterproof servo motors made by Hitec Company and the water jet propellers produced by Raboesch Company. The whole robot is 2.1 kg weight.

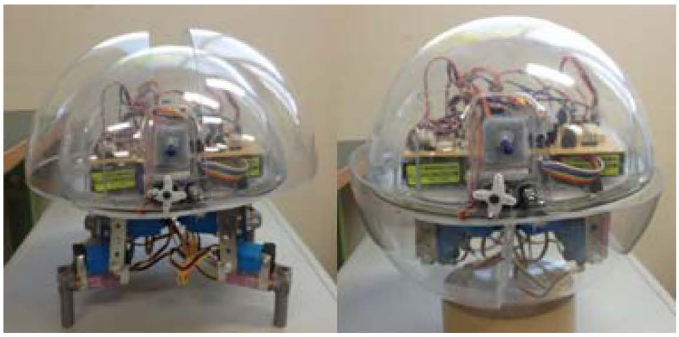

Fig. 4 The prototype spherical mother robot

B. Velocity Experiments in Different Terrains

In order to make the robot to implement practical applications, we did plenty of experiments for the spherical robot in different terrains, not just in the laboratory, including tile floor, asphalt road, cement floor, brick road, sand and

grass. As Fig. 5 shows, these terrains are different in friction coefficient and roughness, so the adaptability on these environments can illustrate that of the robot on a wide range of on-land environments. Also, we evaluated the robot`s walking ability on slope. For evaluating the on-land performance of the spherical mother robot, we implemented three gaits with duty factor of 0.8, 0.75 and 0.67 respectively on the robot.

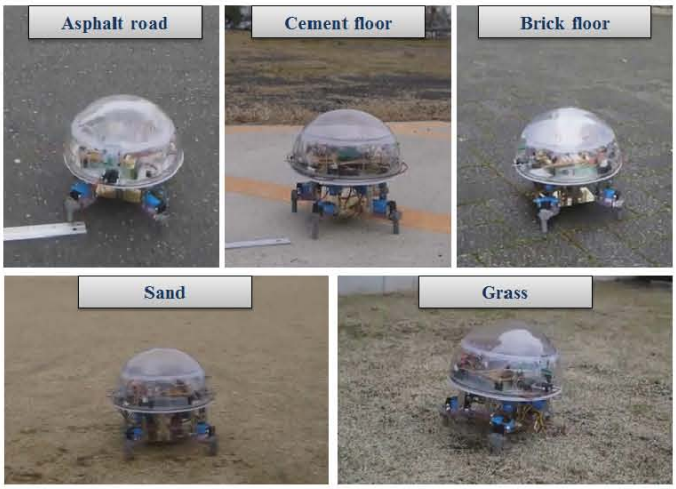

Fig. 5 Walking experiments in different terrains

Fig. 6 indicates the walking velocity of robot in different terrains, including the tile floor in the laboratory, asphalt road, brick road and sand outside. For evaluating the on-land performance, we detected the robot walking velocity under different frequency for different gaits. The blue, red and green points in these figures show the speed of Gait 1, Gait 2 and Gait 3 respectively. As the graphs show, with the frequency increasing, the walking velocity will increase at first and then decrease to zero in each walking gait and each terrain. Under a relatively low frequency, the walking velocities of the robot in one terrain are roughly equal in three kinds of gaits. While under a relatively high frequency, walking velocity increases by changing the gait from Gait 1 to Gait 3.

Fig. 6 (a) shows the experimental results on the tile floor. As the tile floor is a smooth ground, robot can move in a faster speed than on the other grounds. From Fig.6 we know that under a low frequency the walking velocities of the robot are almost the same on four kinds of grounds. With the control frequency increasing, the rougher the ground is, the faster the velocity decreases to zero.

Fig. 7 indicates the theoretical value of robot walking speed under three kinds of walking gaits. By calculating the equation (8), the theoretical value of robot walking speed was gotten. In one kind of walking gait, the theoretical value of walking speed is in proportion to the control frequency and has a linear relationship. Under a given control frequency, the walking speed is in inverse proportion to the duty factor of the gait timing sequences. However, the experimental results show a non-linear relationship between the velocity and frequency. Under a high control frequency, the walking speed is incompletely in inverse proportion to the duty factor of the gait timing sequences, as shown in Fig. 6 (c) and Fig. 6 (d).

By equation (6), we know that the velocity of the robot is related to the step size of the robot and frequency of one step cycle. With the same walking gait, the velocity is distinct under a fixed frequency in four kinds of terrains. Hence, the different step size loss causes different decrease of the speed of the robot.

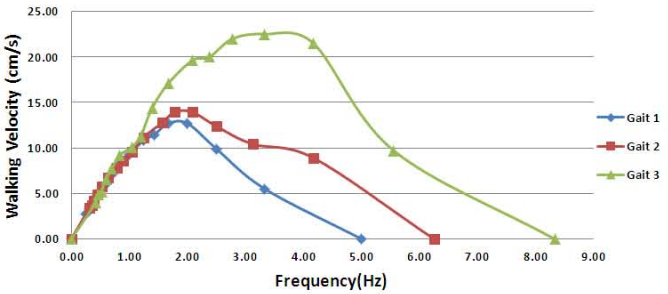

(a) Walking velocity on the tile floor

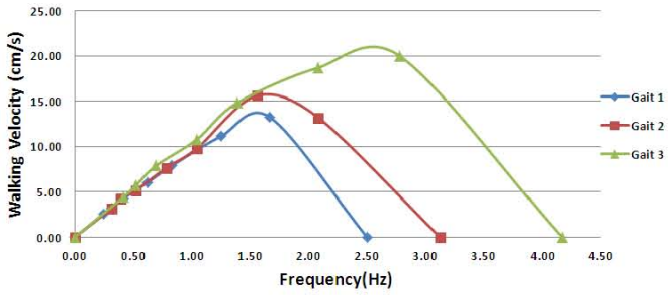

(b) Walking velocity on the asphalt road

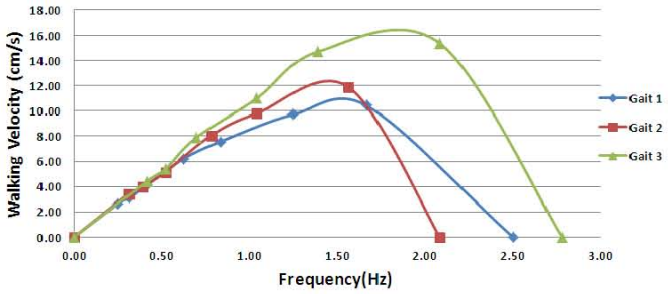

(c) Walking velocity on the brick road

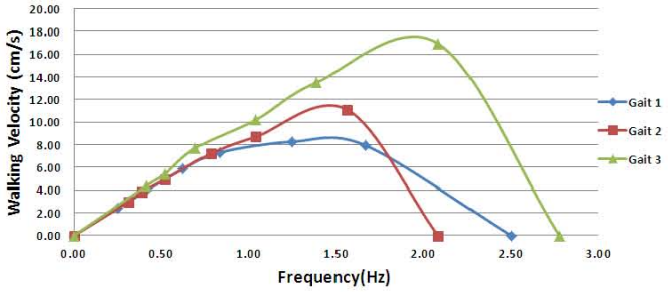

(d) Walking velocity on sand

Fig. 6 Walking experiments in different terrains

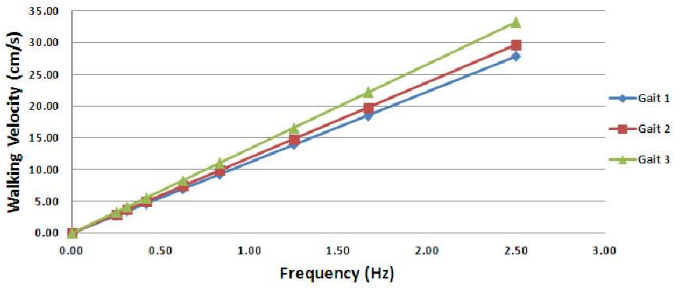

Fig. 7 Theoretical value of robot walking speed in different gaits

By equation (6), the step size of the robot in one step cycle can be calculated. As the step size is in proportion to the rotating angle θ of the leg that is the rotating angle of the horizontal motor, so we set a constant rotating angle 60° for the spherical robot. By the equation (7), with s being equal to 8.5 cm, duty factor β, theoretical value of the step size is calculated as a constant value, $8.898/\beta$ cm.

While, the experimental results of the walking speed in Fig. 8 are not constant values. In a fixed walking gait, the step size increases at first then decreases to zero with the control frequency increasing. That is because that there are three kinds of losses affecting the step size, including the error distance caused by the limited response time of servo motor, which is the main loss, the slip distance between leg and contact surface during one step, and the error distance caused by robot vibrancy. Due to the error distance caused by the limited response time of servo motor, when moving forward, the driving leg moves to the opposite direction before getting the target position under a high control frequency, which causes the decreases reduced to zero.

For the walking forward motion, step size of gait C has the slowest decrease and gait A has the fastest decrease, which is because the on-land phrase of gait C is almost equal to in-air phrase of that. Thus, the actuating ability of servo motor can be fully used under a high control frequency.

Comparing the results among different terrains with the theoretical value, we found that under a low frequency the experimental value is approximately equal to the theoretical value, while under a high frequency there is a big difference between the two values. Under a high frequency, rotating angle error of servo motors exists not only in horizontal direction but also in vertical direction, which is the reason of the decrease of the height of legs in in-air phrase. The rougher the ground is, the faster the leg height decreases. As Fig. 8 shows, in a high frequency, the step size on the roughest ground such as sand and brick road is the shortest, while that on the tile ground is the longest.

To evaluate the robot`s climbing performance on a slope, the experiment was also done. The robot was controlled to climb a slope with wood-made surface. The inclination angle of the slope was measured by a protractor and a plumb bob. We measured the climbing velocity of the robot on the slope with increasing the inclination angle from 0°. Similar to the walking experiments on flat ground, the robot was controlled to move in three gaits. To simplify the experiment, only one frequency was applied for three kinds of gaits. We set a frequency of 0.63Hz for Gait 1, 0.78Hz for Gait 2 and 1.04Hz for Gait 3. The crucial point of climbing a slope is to keep the balance, which means that the robot's center of gravity needs to be maintained inside the polygon formed by the supporting legs.

Fig. 9 shows the climbing experiments results. Although Gait 3 has a higher velocity on a gentle slope, with the slope getting steep, velocity of the robot decreases to zero faster. Gait 2 shows the best performance on a steep slope with the inclination angle of 8°. From the results, Gait 2 is the best walking gait for robot to climb the slope.

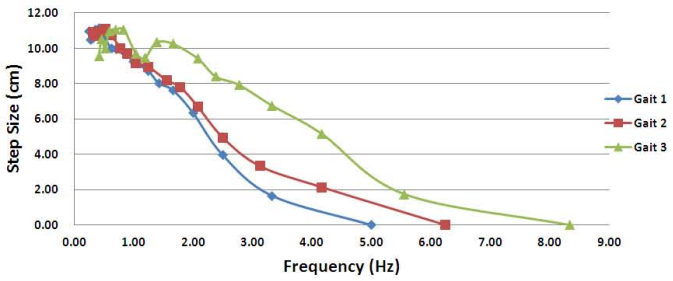

(a) Step size on the tile floor

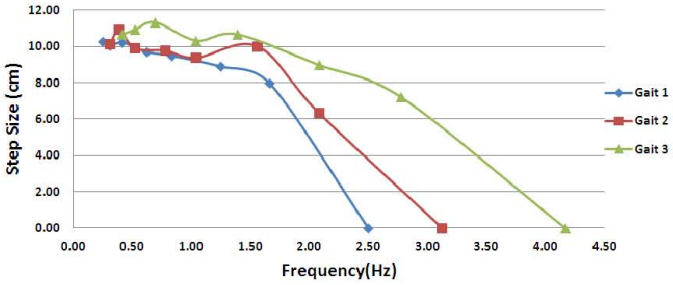

(b) Step size on the asphalt road

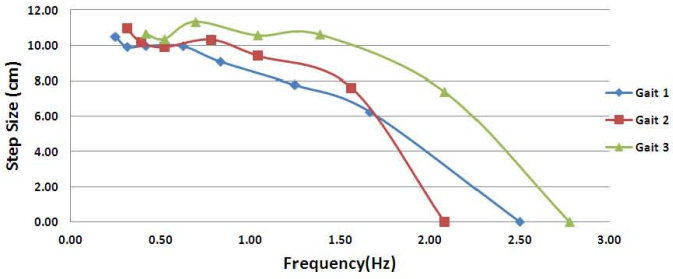

(c) Step size on the brick road

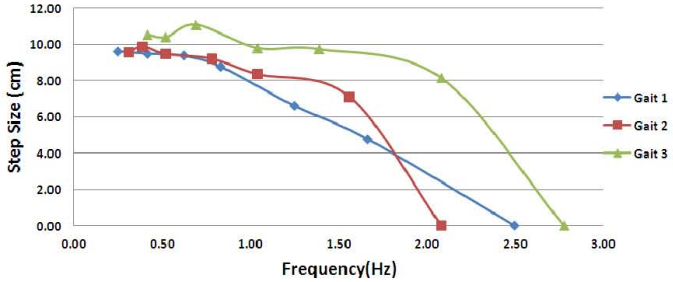

(d) Step size on sand

Fig. 8 Step size of the robot in different terrains

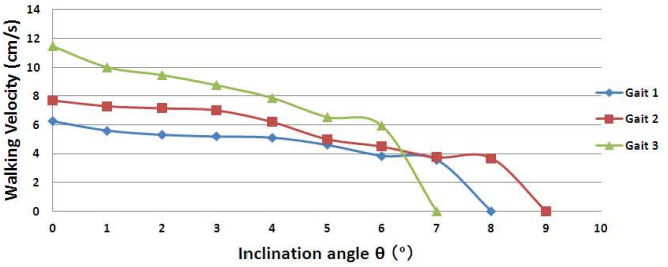

Fig. 9 Climbing experiments on a slope with different inclination angle

V. Conclusions

For making up for the limitations of microrobots, we proposed a mother-son multi-robot system. And we also proposed a novel amphibious spherical robot. The robot can move under a relatively high velocity and in a relatively long time to transport microrobots, on land and under the water. The spherical robot is also used to control and provide the power to microrobots.

In this paper, in order to make the robot to implement practical applications, we did plenty of experiments for the spherical robot in different terrains, not just in the laboratory, including tile floor, asphalt road, cement floor, brick road, sand and grass. And we also did the climbing experiments.

Under a relatively low frequency, the walking velocities in three gaits are roughly equal in each terrain. While under a relatively high frequency, walking velocity increases from Gait 1 to Gait 3. The robot has a higher walking performance on tile floor. Under a control frequency of 3.33 Hz in Gait 3, we got a maximal walking velocity of 22.5 cm/s. For climbing performance, Gait 2 has the best performance on a steep slope with the inclination angle of 8°.

Acknowledgment

This research was supported by the Kagawa University Characteristic Prior Research Fund 2012.

References

[1] W. Zhou, W. Li, "Micro ICPF actuators for aqueous sensing and manipulation", *Sensors and Actuators A: Physical*, Vol. 114, No. 2-3, pp. 406-412, 2004.

[2] L. Shi, S. Guo, and, K. Asaka, "A Novel Jellyfish-Inspired and Butterfly-Inspired Underwater Microrobot with Pectoral Fins", *International Journal of Robotics and Automation*, Vol. 27, No. 3, pp. 276-286, 2012.

[3] P. Brunetto, L. Fortuna, S. Graziani, S. Strazzeri, "A model of ionic polymer–metal composite actuators in underwater operations", *Journal of Smart Material and Structures*, Vol. 17, No. 2, pp. 025-029, 2008.

[4] L. Shi, S. Guo, M. Li, S. Mao, N.Xiao, B. Gao, Z. Song, K. Asaka, "A Novel Soft Biomimetic Microrobot with Two Motion Attitudes", *Sensors*, Vol. 12, No. 12, pp. 16732-16758, 2012.

[5] Q. Pan, S. Guo, T. Okada, "A Novel Hybrid Wireless Microrobot", *International Journal of Mechatronics and Automation*, Vol. 1, No. 1, pp. 60-69, 2011.

[6] S. Kim, I. Lee and Y. Kim, "Performance enhancement of IPMC actuator by plasma surface treatment", *Journal of Smart Material and Structures*, Vol. 16, pp.N6-N11, 2007.

[7] J.J. Gill, K. Ho, G.P. Carman, "Three-dimensional thin-film shape memory alloy microactuator with two-way effect", *J. Microelectromech. Syst.* 11, pp. 68-77, 2002.

[8] Z. Wang, G. Hang, J. Li, Y. Wang, K. Xiao, "A microrobot fish with embedded SMA wire actuated flexible biomimetic fin", *Sensors and Actuators, A 144*, pp. 354-360, 2008.

[9] M. C. Carrozza, A. Arena, D. Accoto, A. Menciassi, P. Dario,"A SMA-actuated miniature pressure regulator for a miniature robot for colonoscopy", *Sensors and Actuators A: Physical*, Vol. 105, No. 2, pp.119-131, 2003.

[10] A. Menozzi, H. A. Leinhos, D. N. Beal, and P. R. Bandyopadhyay, "Open-loop Control of a Multifin Biorobotic Rigid Underwater Vehicle", *IEEE Journal of Oceanic Engineering*, Vol. 33, No. 2, pp. 112-116, 2008.

[11] X. Lin, S. Guo, "Development of a Spherical Underwater Robot Equipped with Multiple Vectored Water-Jet-Based Thrusters", *Journal of Intelligent and Robotic Systems,* Vol. 67, No. 3-4, pp. 307-321, 2012.

[12] U. A. Korde, "Study of a jet-propulsion method for an underwater vehicle", *Ocean Engineering*, Vol.31, No.10, pp.1205-1218, 2004.

[13] K. Watanabe, "An AUV Based Experimental System for the Underwater Technology Education", *Proceedings of Oceans 2006-Asia Pacific*, pp.1-7, 2006.

[14] X. Lin, S. Guo, K. Tanaka, and S. Hata, "Development and Evaluation of a Vectored Water-jet-based Spherical Underwater Vehicle", *INFORMATION: An International Interdisciplinary Journal*, Vol. 13, No. 6, pp. 1985-1998, 2010.

[15] C. P. Santos, V. Matos, "Gait transition and modulation in a quadruped robot: A brainstem-like modulation approach", *Robotics and Autonomous Systems,* Vol. 59, pp.620-634, 2011.

[16] T. Arai, E. Pagello, and L. Parker, "Guest editorial: Advances in multirobot systems", *IEEE Transactions on Robotics and Automation*, Vol. 18, pp. 655-661, 2002.

[17] R. Chase, A. Pandya, "A Review of Active Mechanical Driving Principles of Spherical Robots", *Robotics,* pp. 1 – 21, 2012.

[18] L. Shi, S. Guo, S. Mao, M. Li, and K. Asaka, "Development of a Lobster-inspired Underwater Microrobot", *International Journal of Advanced Robotic Systems*, Vol. 10, No. 44, pp. 1-15, 2013.

[19] D. R. Yoerger, J. GSlotine Cooke, J.E. J. "The influence of thruster dynamics on underwater vehicle behavior and their incorporation into control system design", *IEEE Journal of Ocean Engineering*, Vol.15, No.3, pp. 167-178, 2009.

[20] G. Dudek, P. Giguere, C. Prahacs, S. Saunderson, J. Sattar, L. Torres-Mendez, M. Jenkin, A. German, A. Hogue, A. Ripsman, J. Zacher, E. Milios, H. Liu, and P. Zhang, M. Buehler, C. Georgiades, "AQUA: An Amphibious Autonomous Robot", *Computer*, Vol. 40, No. 1, pp. 46-53, 2007.

[21] C. Zhou, K. Low, "Better Endurance and Load Capacity: An Improved Design of Manta Ray Robot (RoMan-II)", *Journal of Bionic Engineering,* Vol.7, Supplement, pp. 137-144, 2010.

[22] K. Tadakuma, R. Tadakuma, M. Aigo, M. Shimojo, M. Higashimori, M. Kaneko, ""Omni-Paddle": Amphibious Spherical Rotary Paddle Mechanism", Proceedings of *2011 IEEE International Conference on Robotics and Automation*, pp.5056-5062, 2012.

[23] S. Guo, M. Li, L. Shi, S. Mao, "Development of a Novel Underwater Biomimetic Microrobot with Two Motion Attitudes", *Proceedings of the 2012 ICME International Conference on Complex Medical Engineering*, pp. 763-768, 2012.

[24] C. P. Santos, V. Matos, "CPG modulation for navigation and omnidirectional quadruped locomotion", *Robotics and Autonomous Systems*, Vol. 60, No. 6, Pages 912-927, 2012

[25] S. Guo, M. Li, L. Shi and S. Mao, "A Smart Actuator-based Underwater Microrobot with Two Motion Attitudes", *Proceedings of 2012 IEEE International Conference on Mechatronics and Automation*, pp. 1675-1680, 2012.

[26] S. Guo, L. Shi, N. Xiao, and K. Asaka, "A Biomimetic Underwater Microrobot with Multifunctional Locomotion", *Robotics and Autonomous Systems,* Vol. 60, No. 12, pp. 1472-1483, 2012.

[27] V. Loc, I. Koo, D. Tran, S. Park, H. Moon, H. Choi, "Improving traversability of quadruped walking robots using body movement in 3D rough terrains", *Robotics and Autonomous Systems,* Vol. 59, No. 12, pp. 1036–1048, 2011.

[28] S. Guo, M. Li, L. Shi, S. Mao, C. Yue, "Performance Evaluation on Land of an Amphibious Spherical Mother Robot", *Proceedings of the 2013 ICME International Conference on Complex Medical Engineering*, accepted, 2013.

[29] P. Liljebäck, K.Y. Pettersen, Ø. Stavdahl, J.T. Gravdahl. "A review on modelling, implementation, and control of snake robots", *Robotics and Autonomous Systems*, Vol. 60, No. 1, pp. 29–40, 2012.